Surface Modification of Starch Nanocrystals Through Ring-Opening Polymerization of ε-Caprolactone and Investigation of Their Microstructures

Hassan Namazi, Abbas Dadkhah

Research Laboratory of Dendrimers and Nanopolymers, Faculty of Chemistry, University of Tabriz, Tabriz, Iran

Received 22 January 2008; accepted 30 May 2008
DOI 10.1002/app.28821
Published online 18 August 2008 in Wiley InterScience (www.interscience.wiley.com).

ABSTRACT: Bionanoparticles of starch obtained by submitting native potato starch granules to acid hydrolysis conditions. The resulted starch nanoparticles were used as core or macro initiator for polymerization of ε-caprolactone (CL). Starch nanoparticle-*g*-polycaprolactone was synthesized through ring-opening polymerization (ROP) of CL in the presence of $Sn(Oct)_2$ as initiator. The detailed microstructure of the resulted copolymer was characterized with NMR spectroscopy. Thermal characteristic of the copolymer was investigated using DSC and TGA. By introducing PCL, the range of melting temperature for starch was increased and degradation of copolymer occurred in a broader region. X-ray diffraction and TEM micrographs confirmed that there was no alteration of starch crystalline structure and morphology of nanoparticles, respectively. © 2008 Wiley Periodicals, Inc. J Appl Polym Sci 110: 2405–2412, 2008

Key words: nanoparticles; biopolymers; ring-opening polymerization; microstructure; graft copolymers; polyesters

INTRODUCTION

Application of renewable resources such as starch to synthesis biodegradable polymers with desired physicochemical and biological properties has recently received increasing interests because of their abundant availability, low costs, renewability, and no toxicity of these kind of material.[1–7] Starch is a natural, renewable, high polyol, available in plenty, and hence in low cost. It usually has two major components and appears as a mixture of two glucosidic macromolecules very different in structure and properties: largely linear amylose of molecular weight between 1000 and 1,000,000, consisting of α-(1-4)-linked D-glucopyranose and amylopectin, having the same backbone as amylose but with a large number of α-(1-6)-linked branch points.[8] Native starch occurs in the form of discrete and partially crystalline microscopic granules that are held together by an extended micellar network of associated molecules.

On the other hand, with the highlight of using nanomaterials in research fields, considerable efforts have gone into the development of bionanoparticles from the biopolymers.[9] Some of the polysaccharides such as starch are potential renewable sources of nano sized state.[10] It is well known that the native starch granules contain more or less concentric "growth ring" or shells or layers that are readily visible by optical or electron microscopy. The molecular chain of amylose almost is perpendicular to these growth rings and to the surface of the granules. This onion-like structure has been attributed to the chemical differences between the layers, differences in the density of deposition of molecules of starch, and differences in crystallinity.[11] Aqueous acids can be employed to hydrolyze the amorphous sections found in these naturally occurring polysaccharides. Consequentially crystalline section of polymers is released, resulting in individual mono crystalline bionanoparticles. The object of this treatment is to dissolve away regions of low lateral order so that the water insoluble, highly crystalline residue may be converted in to a stable suspensoid by subsequent vigorous mechanical shearing action.

Graft copolymerization, as a reasonable approach of chemical modification, has been extensively used in the modification of starch.[12–18] Recently, some new development for modification of starch nanoparticles to prepare nano scale materials as the reinforcer in nanocomposites and also their utilization for application in medical field has been received a lot of interests.[19–25] It is well known that starch can generate graft copolymers with variety of vinyl monomers. The graft polymerization of polyesters such as PLA and PCL has been prepared through chemical methods usually via ring-opening polymerization (ROP) and using chain extenders.[26–28]

Correspondence to: H. Namazi (namazi@tabrizu.ac.ir).

Isocyanates, such as 2,4-tolylene diisocyanate (TDI), methylenediphenyl diisocyanate (MDI), were previously investigated as chain extender in graft copolymerization of starch and starch nanoparticles. However, isocyanates are considered as environmentally hazardous materials.[12]

Our purpose in this work is synthesizing the new graft copolymer with well defined structure based on starch nanoparticles and ε-caprolactone (CL) via ROP graft polymerization. This method not only offers an effective and safe way for chemical modification but also could develop fully biodegradable material with potential application in medical applications.

EXPERIMENTAL

Materials

Potato starch was purchased from Fluka and was dried at 110°C for about 10 h to remove absorbed moisture. ε-CL obtained from Aldrich and was dried over calcium hydride for 2 days and distilled under reduced pressure. $Sn(Oct)_2$ was purchased from Aldrich and was used as received without further purifications. All other chemicals were analytical grade and were used as received.

Measurements

NMR spectroscopy

NMR spectra analysis was recorded on a Bruker 400 MHz for a carbon 13 isotope. Sample was dissolved in DMSO at 60°C, and the solution concentration was 15% w/v. The spectra were obtained at 60°C with a pulse angle of 30°, a delay time of 10 s and an acquisition time of 2 s. All of the chemical shifts are reported in parts per million (ppm) using HMDS as references, which is usually used as an internal standard for NMR measurements at elevated temperature.

FTIR

The FTIR analysis was performed using a FTIR Bruker-Tensor 270 spectrometer. The starch nanocrystals were mixed with analytical grade KBr at a weight ratio of 5/200 mg.

XRD

The pattern of X-ray diffraction of the samples was obtained by Siemens diffractometer with Cu-Kα radiation at 35 kV in the scan range of 2θ from 2° to 30°.

Scanning electron microscopy

Scanning electron micrographs were obtained with a LEO 440i scanning electron microscope under vacuum at an operating voltage of 10 kV. Dried starch sample was gold coated by sputtering for 15 s.

Transmission electron microscopy

Transmission Electron Microscopy (TEM) observations were performed using a LEO 906 microscope with an 80 KV voltage, and micrographs were recorded on Kodak film.

Differential scanning calorimetery

Differential Scanning Calorimetery (DSC) measurements accomplished with a Linseis DSC L 63/45 instrument calorimeter. Samples were heated with a heating rate of 10°C min^{-1}.

TGA

TGA carried out on D. T. G. 60 AH Shimadzu instruments. Thermal degradation behavior of samples was studied by thermo gravimetric analysis (TGA) under N_2 flow at a heating rate of 20°C/min.

Preparation of starch nanoparticles

Starch nanocrystals were obtained through Dufresne et al. method.[11] Starch nanocrystals were processed by acid hydrolysis of the amorphous domains of potato starch granules. They occur as a finely divided white powder, insoluble in water. Starch granules 50 g was first mixed with 1 L of 2.2*N* hydrochloric acid (820 mL of water and 180 mL of 36% hydrochloric acid). The nanocrystal suspension (5% w/w of solid component in water) was stored at 35°C for 15 days. Duration of this time allows us to remove most of the amorphous zones without damaging the crystalline zones. The above suspension was stirred all of time to ensure the homogeneity of the suspension. It was then diluted with an equal volume of distilled water and washed by successive centrifugation (4000 trs/min) until acid free. At this step, crystals are broken into nanocrystals, which change the refractive index of the solution so that the suspension becomes opaque. The dispersion of nanocrystals was completed by a further 3 min ultrasonic treatment.

Polymerization procedures

In situ ROP of ε-CL catalyzed by $Sn(Oct)_2$

Starch nanoparticle-*g*-PCL was synthesized as described below. The reaction took place in a 25 mL three-necked flask equipped with a mechanical stirrer and a rubber septum and previously purged with nitrogen. A mixture of starch nanoparticle (1 g) and CL (2 mL) was first added to flask, and the

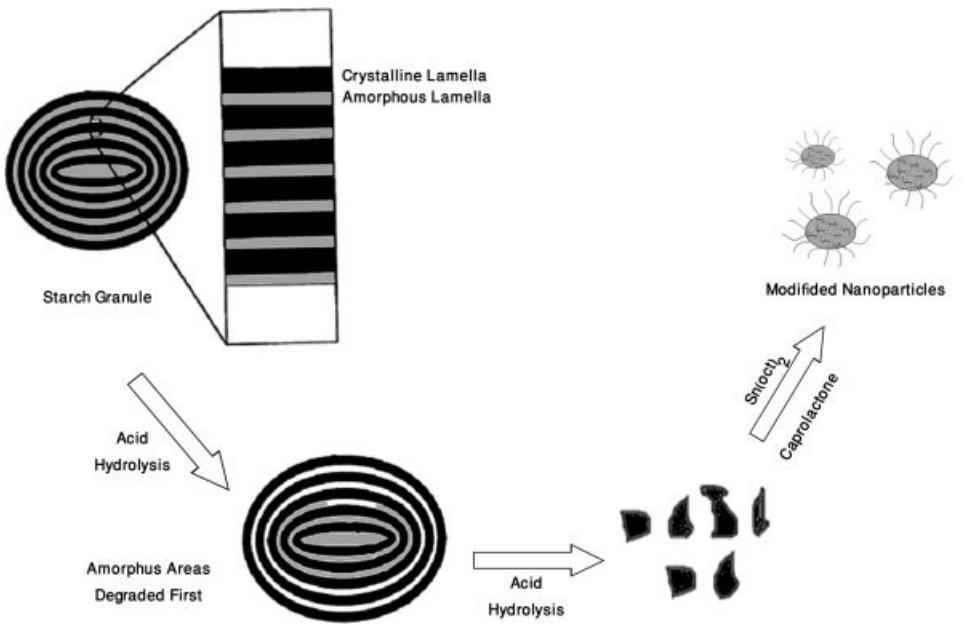

Scheme 1 Typical process for preparation of starch nanocrystal-*g*-PCL from granular potato starch.

temperature of system was adjusted at 75°C. A determined amount of $Sn(Oct)_2$ (0.2% w/w of total amount of reagents) was then introduced via a conditioned syringe. Polymerization was stopped by fast cooling to room temperature.

Separation of homopolymer

Starch nanocrystal-*g*-PCL copolymer and PCL homopolymer might coexist in the reaction product of PCL-modified starch nanocrystal (starch nanocrystal-*g*-PCL). They were separated by toluene extraction. Two grams of the PCL-modified starch nanocrystal was put into a 50 mL toluene in a bottle then the mixture was stirred at 20°C for 24 h and then filtrated. The remaining solids were then washed with toluene for three times. The above process was repeated once again. The filtrates were collected together, concentrated to proper extent, precipitated into *n*-heptane, and dried in vacuum.

RESULTS AND DISCUSSION

Synthesis of starch nanoparticle and starch nanoparticle-*g*-PCL

Polycaprolactone-grafted starch nanoparticle substrate was synthesized from bulk monomer, ε-CL, and in the presence of starch nanoparticle by an *in situ* ring-opening polymerization, to result starch with chemical grafting. Pathway was used, as represented by the reaction shown in Scheme 1. In this method, ROP of CL was carried out by using a Lewis acid catalyst tin octanoate in the presence of starch nanoparticles. Initiation of the ring opening was expected to precede from the hydroxyl groups from the starch phase. Indeed, even though the mechanism of ROP catalyzed by $Sn(Oct)_2$ is not yet well understood; however, it is well established that the actual initiation species are hydroxyl-containing compounds, e.g., alcohol or residual water. In addition to chemical grafting of the PCL chains onto starch nanoparticles, an improvement of adhesion was also expected by the fact that the polyester chains are growing in close contact to the starch nanoparticle phase.

Characterization of starch nanoparticle-*graft*-PCL

FTIR analysis

Figure 1 shows the spectra of pure starch nanocrystals (A) as well as starch nanocrystal-*g*-PCL (B). From comparison of FTIR spectra of product (B) and starch nanocrystal (A) in Figure 1, the main difference between Spectrum A and Spectrum B is a peak at 1734 cm^{-1} as the characteristic of the ester group related to PCL on starch. The intensity of hydroxyl stretching groups in starch nanocrystal (3400 cm^{-1}) was slightly decreased in the spectrum (B). The characteristic peaks at 1734 and 3400 cm^{-1} in Spectrum B illustrate that the starch nanocrystals have initiated the polymerization of the ε-CL, and the surface of the starch nanoparticles have been grafted by CL; our desirable product (starch nanoparticle-*g*-PCL) was formed.

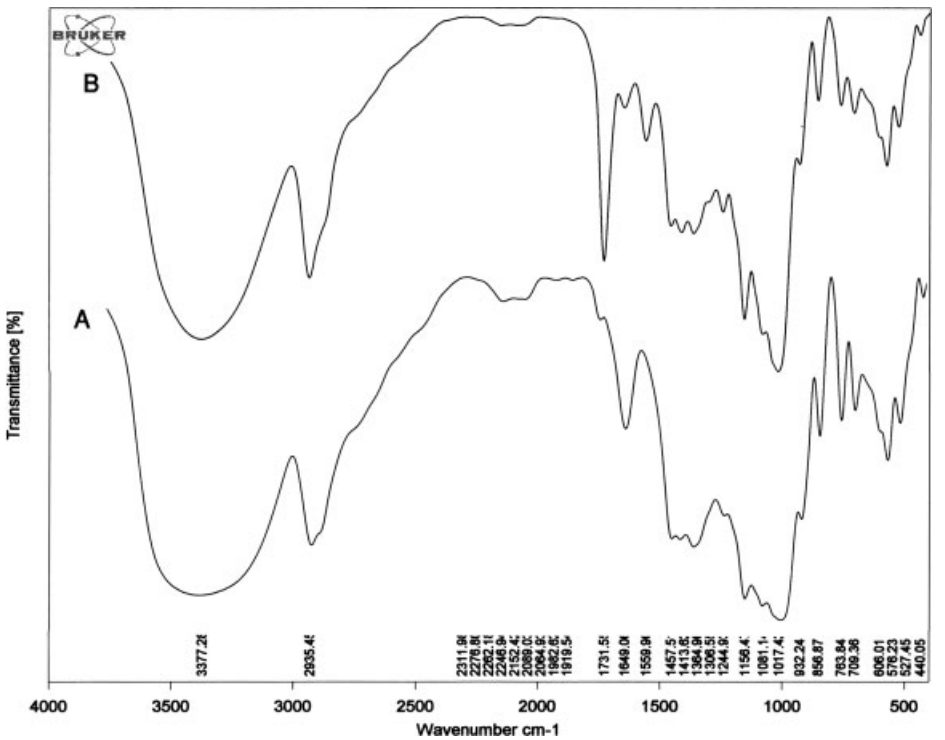

Figure 1 FTIR spectrum of (A) unmodified starch nanocrystal and (B) starch nanocrystal-*g*-PCL.

NMR analysis

The structure of synthesized starch nanoparticle-*g*-PCL was confirmed by ^{1}H and ^{13}C NMR. The analysis for starch nanocrystal-*g*-PCL was performed at 25 and 60°C. From comparison of patterns in Figure 3 it was found that in higher temperatures the peaks become sharper. It is probably due to increased solubility of copolymer in higher temperatures. Based on the peak assignments in literature[29–31] for proton species in amylose, amylopectin, starch, and starch derivatives with similar chemical environments to starch nanocrystal-*g*-PCL, here the proton signals in the obtained ^{1}H NMR spectrum of starch nanocrystal-*g*-PCL was assigned as quoted in Table I. Also, the ^{13}C NMR spectrum assignments of starch nanocrystal-*g*-PCL are shown in Table I, whereas the glucopyranan carbons are between 60 and 101 ppm. Numbers 1–6 denoted the carbons in the starch nanocrystals unit, and the Greek symbols indicate the carbons in CL unit as illustrated in Figure 2. From consideration of data in Table I, it is found that C_1 and C_6 carbons have connected with two kinds of protons, denoted by the subscripts a and b, respectively. Because this type of peak splitting is also observed in the case of pure starch, it is pointed out that this is not originated from the formation of PCL graft. Thus, $H_{1,a}$ and $H_{6,a}$ were assigned to the protons attached to the main C_1 and C_6 carbons; whereas, $H_{1,b}$ and $H_{6,b}$ were assigned to the protons linked to the C_1 and C_6 carbons in the branch point

TABLE I
Chemical Shift Assignments for ^{1}H and ^{13}C NMR of Starch Nanocrystal-*g*-PCL

^{13}C assignment	Chemical shift (ppm)	^{1}H NMR assignment	Chemical shift (ppm)
C_α	33.18	$H_{\alpha,a}$	2.17
		$H_{\alpha,b}$	2.27
C_β	24.93	H_β	1.29
C_γ	24.15	H_γ	1.53
C_δ	26.55	$H_{\delta,a}$	1.54
		$H_{\delta,b}$	1.40
C_ε	63.20	$H_{\varepsilon,a}$	3.97
		$H_{\varepsilon,b}$	3.37
C=O	172.59		
C_1	99.81	$H_{1,a}$	5.11
		$H_{1,b}$	5.03
C_2	73.00	H_2	3.66
C_3	71.83	H_3	3.30
C_4	78.68	H_4	3.36
C_5	71.39	H_5	3.60
C_6	60.36	$H_{6,a}$	3.66
		$H_{6,b}$	3.60

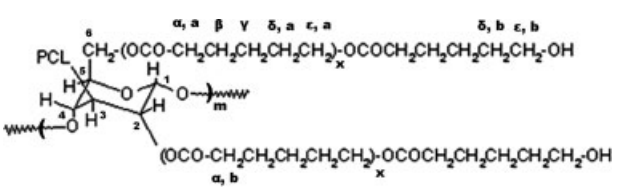

Figure 2 Molecular structure of synthesized copolymer.

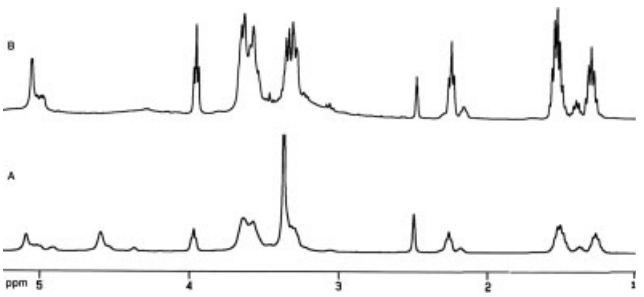

Figure 3 ^{1}H NMR spectra of starch nanocrystal-*g*-PCL in DMSO-d_6 (A) in 25°C and (B) in 60°C.

of amylopectin unit. The C_α, C_δ, and C_ε carbons in the PCL grafts also have two corresponding protons, respectively. However, unlike the case of starch, these are induced by the differences in chemical environment between the corresponding protons. That is, the $H_{\alpha,a}$ can be assigned to the methylene proton in the type of —CH_2(OC=O)CH_2— linkage appearing at the internal α-position of the graft chain, and the α-methylene unit at the initiating site of the graft from the C_6 carbon of the starch. On the other hand, the $H_{\alpha,b}$ corresponds to the methylene proton in the —CH_2(OC=O)CH_2— type linkage, which is present at the initiating site of the grafts from C_2 to C_3 carbons of the starch. A similar assignment is also possible for H_δ or H_ε protons. The $H_{\delta,a}$ and $H_{\varepsilon,a}$ protons indicate the internal δ- and ε-methylene protons, respectively. In the —CH_2CH_2(OC=O)C— type linkage, whereas the $H_{\delta,b}$ and $H_{\varepsilon,b}$ protons are the methylene protons attached to the hydroxyl end in the —CH_2CH_2OH unit of each PCL graft. These detailed assignments are also shown in Figure 2.

Quantitative analysis of the microstructure of starch nanocrystal-*g*-PCL

Proton NMR spectroscopy is one of the most powerful tools for the quantitative analysis in the polymer microstructure based on the polymer peak assignment of starch ring protons. As shown in Table I, based on the peak assignment of glucosidic rings in the starch nanocrystal as well as CL unit the microstructure of starch nanocrystal-*g*-PCL was analyzed by calculation with taking into account the peak intensity in ^{1}H NMR spectra. The composition of starch nanocrystal-*g*-PCL as well as DS values and DP values were analyzed by means of the quantitative ^{1}H NMR spectra.

To determine relative mol fraction (CL/starch nanocrystall) of starch nanocrystal and CL units in the graft copolymer, the signals around 3.6–3.7 ppm containing H_2, H_5, and H_6 protons for starch nano unit and signals in the 1.3–2.7 ppm region containing α–δ methylene protons for CL unit were selected. Therefore, mole fraction of sample can be assigned as follows:

$$\frac{\text{Caprolactone}}{\text{Starch}} = \frac{\text{Intensity average of } \alpha-\delta \text{ methylene proton signals}}{\text{Intensity average of } H_2, H_5 \text{ and } H_6 \text{ proton signals}}$$

NCL, which is the total number of grafted CL units per 100 anhydroglucose units in starch nanocrystal, also could be obtained by simple calculation, NCL = CL/St × 100.

To obtain the more detailed graft structure of starch-*g*-PCL, we considered the structural differences between the C_2- and C_3-branches and the C_6-branch. The starting protons of the C_2- and C_3-branches are composed of —CH(OC=O)CH_2— units that are assigned as α-methylene proton $H_{\alpha,b}$. However, the starting proton of the C_6 branch cannot be distinguished from the main CL units due to its identical structure of the type —CH_2(OC=O)CH_2—, which is denoted by $H_{\alpha,a}$. Thus, the fraction of CL units at the starting site of C_2- and C_3-branches can be calculated by $F_{\alpha,b} = I_{\alpha,b}/(I_{\alpha,a} + I_{\alpha,b})$, whereas $I_{\alpha,a}$ and $I_{\alpha,b}$ represent the ^{1}H NMR signal intensities of $H_{\alpha,a}$ and $H_{\alpha,b}$, respectively. Because the NCL is already known, the number of $C_{2\text{-}}$ and $C_{3\text{-}}$ branches per 100 anhydroglucose units, denoted by $NG_{2,3}$, can be obtained by the simple multiplication, NCL × $F_{\alpha,b}$.

A similar calculation is possible for δ-methylene groups in the end units of $C_{2\text{-}}$, $C_{3\text{-}}$, and $C_{6\text{-}}$branches. The fraction of δ-methylene groups in the CL end units of all grafts having the —CH_2CH_2OH structure can be calculated by: $F_{\delta,b} = I_{\delta,b}/(I_{\delta,a} + I_{\delta,b})$, where $I_{\delta,a}$ and $I_{\delta,b}$ represent the NMR signal intensities of the $H_{\delta,a}$ and $H_{\delta,b}$ protons. Therefore, we can obtain the total number of PCL grafts per 100 anhydroglucose units, NG, and number of $C_{6\text{-}}$branches per 100 anhydroglucose units, NG_6, as follows:

$$NG = NCL \times F_{\delta,b}$$

$$NG_6 = NG - NG_{2,3}$$

Although $NG_{2,3}$ could be distinguished from NG_6, the degree of graft polymerization (DGP) could not be obtained separately for each PCL branch because all of the main CL units in $C_{2\text{-}}$, $C_{3\text{-}}$ and $C_{6\text{-}}$ branches showed similar chemical shifts in NMR spectra. Thus, the average DGP was calculated by the simple equation, DGP = NCL/NG.

By using this method, the calculated values for $F_{\alpha,b}$, $F_{\delta,b}$, NG, $NG_{2,3}$, NG_6, and DGP in the synthesized copolymer were: 0.18, 0.27, 28.14, 19.22, 8.92, and 3.70, respectively; the calculated weight

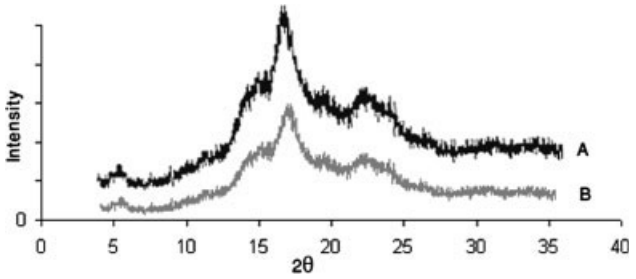

Figure 4 X-ray diffraction patterns of (A) unmodified starch nanocrystal and (B) satrch nanocrystal-*g*-PCL.

fractions by this method showed 39.9% for PCL and 60.1% for starch nanocrystal.

X-ray diffraction study

Starch is a biosynthesized compound containing semicrystalline granules with varying polymorphic types and degree of crystallinity. Polymorphism of the α-glucans is one of the main characteristics of the crystalline parts in starch granules. Because native starch granules contain crystalline regions as shown by their unique X-ray diffraction patterns (XRD), and therefore, granular crystallinity also can be studied with X-ray diffraction technique.

As shown in Figure 4(A) the hydrolyzed unmodified potato starch nanocrystal shows the expected diffraction pattern for the B allomorph: the strong peak at 2θ 17.05 (d = 5.2 Å), a medium intensity peak at 2θ 15.01 (d = 5.9 Å), and medium intensity peaks at 2θ 19.72 (d = 4.5 Å), 22.22 (d = 4.0 Å), and 24.04 (d = 3.7 Å). And as a final remark, we noticed that the peak at 2θ 5.6 (d = 15.8 Å) could be considered as a "finger print" for B-type structure. Comparing the X-ray diffraction of starch nanocrystals before and after acid hydrolysis, it is found that the acid hydrolysis did not destroy or transform the native crystalline state of the nanocrystals.

After modification of starch nanocrystals with polycaprolactone, it is appeared that the crystalline nanoparticle structure is kept intact. The basic B-allomorph diffraction pattern is still clearly visible in the diffraction pattern of the modified nanoparticles, [see Fig. 4(B)]. However, in the XRD pattern of starch nanoparticles, no peak was observed after modification corresponding to crystalline phase of PCL, (PCL shows two main diffraction peak at 2θ 21.5 and 23.9) and this is in agreement with obtained results from DSC observations.

Thermal properties of graft copolymer

TGA analysis

The thermal stability behavior for starch, starch nanocrystal, and starch nanoparticle-*g*-PCL are

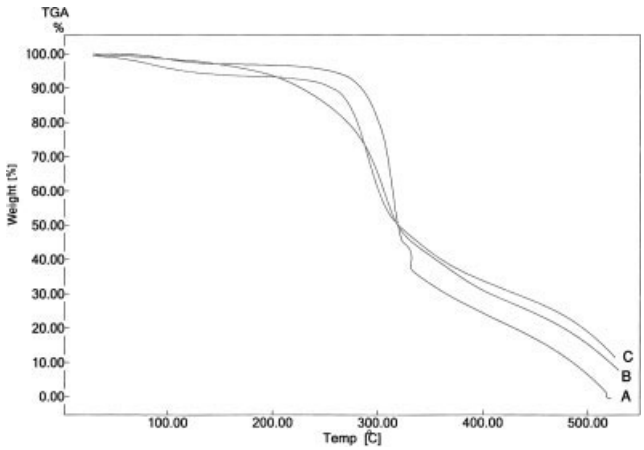

Figure 5 TGA thermograms of (A) starch, (B) starch nanocrystal, and (C) starch nanocrystal-*g*-PCL.

measured by TGA. As shown in Figure 5, the degradation temperature (T_d) was found around 290°C for starch [Fig. 5(A)] and degradation progressed at a narrow temperature range 290–310°C. However, after acidic hydrolysis and disruption of amorphous zone of granules and production of starch nanoparticles, the thermal stability decreased [Fig. 5(B)] but still progressed at a narrow temperature range 285–300°C. However, degradation of starch nanoparticles grafted PCL continued in broader temperature range 220–310°C [Fig. 5(C)]. On the other hand, the degradation of starch nanocrystal-*g*-PCL shifted to lower temperature and continued to be slower than unmodified starch nanoparticles.

The typical DSC curves for starch nanocrystal [Fig. 6(A)] and starch nanocrystal-*g*-PCL [Fig. 6(B)] are collected in Figure 6. The PCL homopolymer has a T_m at 61°C, and starch nanocrystal has T_m in the region between 112 and 240°C, whereas starch nanocrystal decomposition occurs above 240°C. PCL

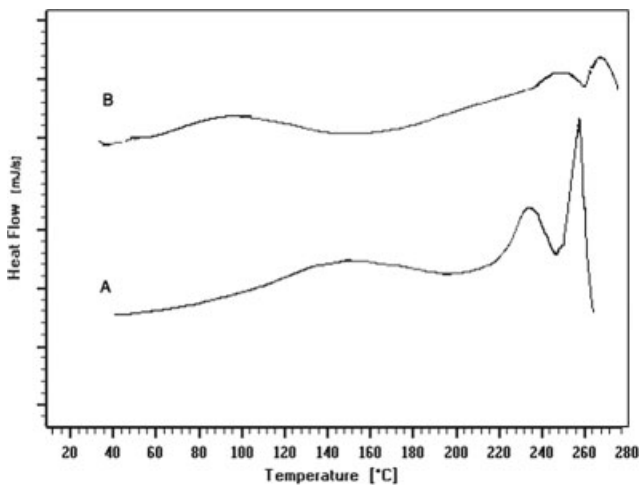

Figure 6 DSC thermograms of (A) starch nanocrystal and (B) Starch nanocrystal-*g*-PCL.

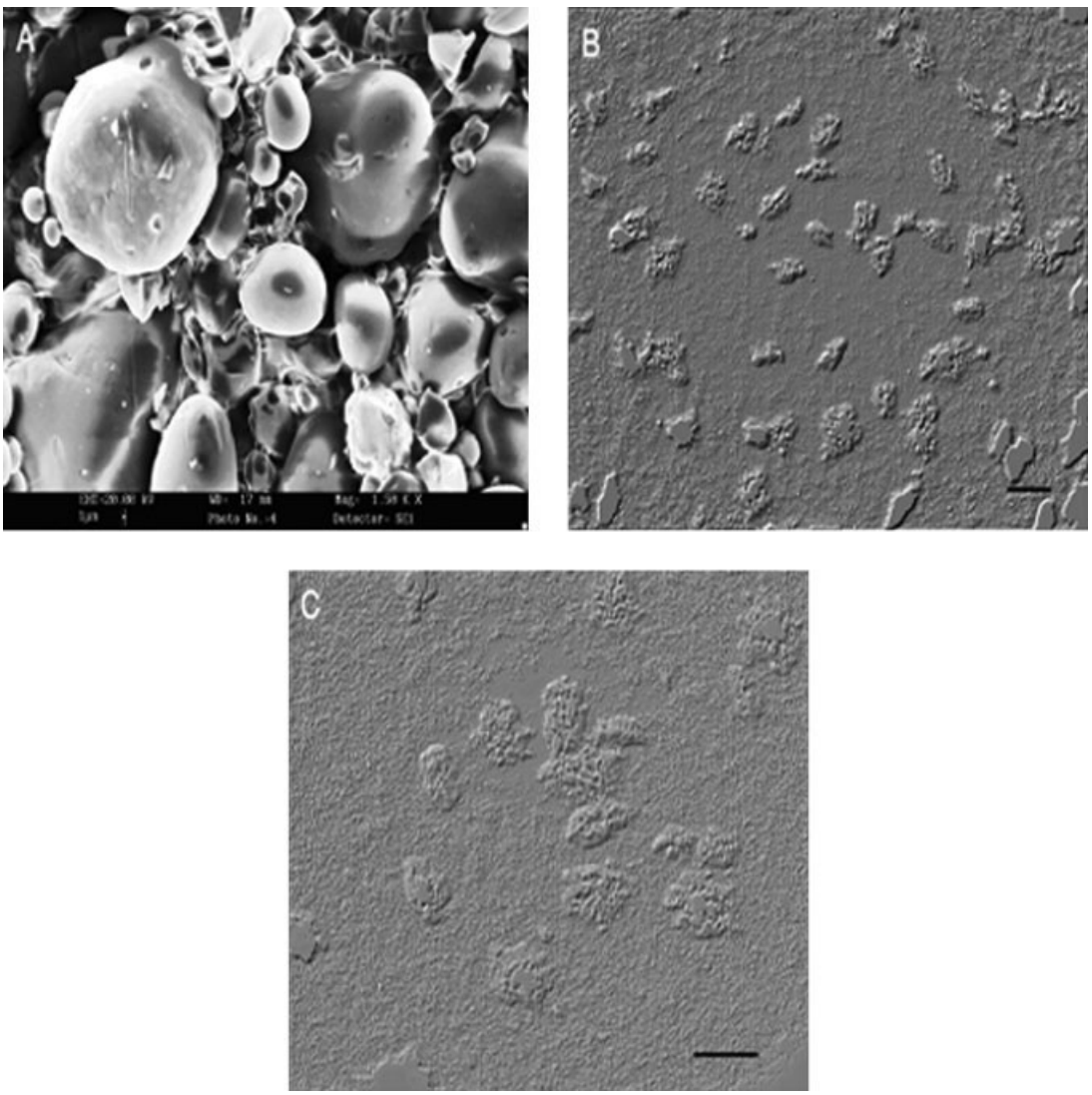

Figure 7 SEM micrograph of (A) starch granule and (B) TEM photograph of starch nanocrystals before and (C) after chemical modification. Scale bar: 200 nm.

modified starch nanocrystal did not show a separate melting signal in its DSC thermograms even though the melting point of polycaprolactone was significantly lower than any starch signal. The absent of a clear PCL signal of crystalline PCL phase is an indication of the absence of a crystalline PCL phase at the starch nanocrystal surface.

Also, we were able to determine theoretically the weight fraction of both starch and grafted polymer in comparison with the melting energies associated with grafted and ungrafted starch nanoparticles from DSC thermograms. However, the integration of the corresponding peak and its dissociation from any phenomenon associated with the grafted polymer layer are difficult to estimate so that the exact melting enthalpy of starch nanocrystals cannot be easily determined. The starch weight content can be obtained by dividing the total enthalpy associated with the melting process for the grafted nanoparticles through the corresponding enthalpy for the ungrafted nanoparticles. The grafting efficiency presumption from DSC analysis is mainly a qualitative procedure.[21]

Morphological observation

SEM and TEM were used to investigate the possible morphological changes of starch granules during hydrolysis. Figure 7(A) shows SEM micrograph of starch before hydrolysis.

A typical electron micrograph obtained from the dilute suspension of hydrolyzed starch before and after chemical modification is shown in Figure 7(B,C), respectively. In the case of unmodified starch nanoparticles, the suspension is constituted of starch fragments which have a homogenous distribution in

size. Each fragment is constituted of associated nanocrystals, which are not clearly identified and also in the modified starch nanocrystals. The surface of nanocrystals looks smooth, whereas the surface of the starch nanocrystal-*g*-PCL exhibits roughness and some connection between nanoparticles, which is clearly seen. Therefore, it was concluded that the PCL was located on the surface of the starch nanoparticles. It seems that they have been coated with a polymeric layer because of their size increase in comparison to ungrafted particles.

CONCLUSIONS

The graft polymerization of CL monomer onto isolated starch nanoparticles was conducted. Successful surface modification was confirmed using FTIR and NMR spectroscopy. Molecular weight and frequency of PCL moieties on the C_2, C_3, and C_6 hydroxyl groups of glycosidic unit of starch nanoparticle was calculated by means of NMR. Weight fraction of construction component of graft copolymer was also calculated by NMR. XRD and DSC analysis showed that the crystalline structure of starch nanocrystals do not change during chemical modification. It seems that chemical modification causes the decomposition of copolymer in the broader rang of temperature rather than unmodified starch nanocrystals. TEM observation also confirmed the existence of CL on the surface of starch nanoparticles.

We would like to thank Department of Physics and Department of Material Engineering in the University of Tabriz for XRD analysis and SEM Images and SUT for TGA analysis.

References

1. Kim, D. H.; Lee, S. H.; Im, K. N.; Kim, K. N.; Kim, K. M.; Shim, I. B.; Lee, M. H.; Lee, Y. K. Curr Appl Phys 2006, 6S1, e242.
2. Alexiou, C.; Arnold, W.; Hulin, P.; Klein, R. J.; Renz, H.; Parak, F. G.; Bergemann, C.; Lubbe, A. S. J Magn Magn Mater 2001, 225, 187.
3. Echeverria, I.; Silva, I.; Gurruchaga, G. M. J Appl Polym Sci 2005, 96, 523.
4. Geresh, Sh.; Gilboa, Y.; Korol, J.; Gdalevsky, G.; Voorspoels, J.; Remon, J. P.; Kost, J. J Appl Polym Sci 2002, 86, 1157.
5. Jihuai, W.; Yueling, W.; Jianming, L.; Songbai, L. Polymer 2003, 44, 6513.
6. Sun, G.; Feng, J.; Jing, F.; Pei, F.; Liu, M. J Magn Magn Mater 2003, 265, 123.
7. Chen, L.; Xie, Z.; Zhuang, X.; Chen, X.; Jing, X. Carbohydr Polym 2008, 72, 342.
8. Chakraborty, S.; Sahoo, B.; Teraoka, I.; Gross, R. A. Carbohydr Polym 2005, 60, 475.
9. Angellier, H.; Choisnard, L.; Molina-Boisseau, S.; Ozil, P.; Dufresne, A. Biomacromolecules 2004, 5, 1545.
10. Fang, J. M.; Fowler, P. A.; Hill, C. A. S. J Appl Polym Sci 2005, 96, 452.
11. Dufresne, A.; Cavaille, J. Y.; Helbert, W. Macromolecules 1996, 29, 7624.
12. Gong, Q.; Wang, L. Q.; Tu, K. Carbohydr Polym 2006, 64, 501.
13. Chen, L.; Ni, Y.; Bian, X.; Qiu, X.; Zhuang, X.; Chen, X.; Jing, X. Carbohydr Polym 2005, 60, 103.
14. Cho, C. G.; Lee, K. Carbohydr Polym 2002, 48, 125.
15. Athawale, V. D.; Lele, V. Carbohydr Polym 2000, 41, 407.
16. Zhai, M.; Yoshii, F.; Kume, T.; Hashim, K. Carbohydr Polym 2002, 50, 295.
17. Fanta, G. F.; Felker, F. C.; Shogren, R. L. Carbohydr Polym 2004, 56, 77.
18. Lee, J. S.; Kumar, R. N.; Rozman, H. D.; Azemi, B. M. N. Carbohydr Polym 2004, 56, 347.
19. Chakraborty, S.; Sahoo, B.; Teraoka, I.; Miller, L. M.; Gross, R. A. Macromolecules 2005, 38, 61.
20. Angellier, H.; Molina-Boisseau, S.; Belgasem, M. N.; Dufresne, A. Langmuir 2005, 21, 2425.
21. Thielemans, W.; Belgacem, M. N.; Dufresne, A. Langmuir 2006, 22, 4804.
22. Labet, M.; Thielemans, W.; Dufresne, A. Biomacromolecules 2007, 8, 2916.
23. Angellier, H.; Molina-Boisseau, S.; Dole, P.; Dufresne, A. Biomacromolecules 2006, 7, 531.
24. Angellier, H.; Molina-Boisseau, S.; Lebrun, L.; Dufresne, A. Macromolecules 2005, 38, 3783.
25. Angellier, H.; Molina-Boisseau, S.; Dufresne, A. Macromolecules 2005, 38, 9161.
26. Mani, R.; Tang, J.; Bhattacharya, M. Macromol Rapid Commun 1998, 19, 283.
27. Kweon, D. K.; Cha, D. S.; Park, H. J.; Lim, S. T. J Appl Polym Sci 2000, 78, 986.
28. Xu, Q.; Kennedy, J. F.; Liu, L. Carbohydr Polym 2008, 72, 113.
29. Choi, E. J.; Kim, C. H.; Park, J. K. Macromolecules 1999, 32, 7402.
30. Nilsson, G. S.; Bergquist, K. E.; Nilsson, U.; Gorton, L. Starch/Starke 1996, 48, 352.
31. Largnel, B.; Bliard, C.; Massiot, G.; Nuzillard, J. M. Carbohydr Res 1997, 298, 251.